SLOPE FAILURE ANALYSIS WITH STRENGTH REDUCTION IN OPENGEOSYS

A PREPRINT

Tengfei Deng, Thomas Nagel

January 21, 2021

ABSTRACT

The stability of slopes plays an important role in geotechnical engineering. In this paper, an example of a slope stability analysis is described in OpenGeoSys using the strength reduction technique. The results are compared with those calculated by other software. The simulation results agree well, indicating that the method used in OpenGeoSys is a valid approach.

Keywords Safety Factor · Slope Stability · Strength Reduction · OpenGeoSys

1 Introduction

Slope stability analysis is a classic problem in slope engineering research. Factor of safety and the failure pattern of the slope are the most significant technical indicators that need to be considered in the safety assessment of a slope. The aim of this technical note was to apply the strength reduction method in OpenGeoSys for analyzing slope stability using the Mohr-Cloulomb material model based on corner and apex smoothing [1, 2] implemented using the MGIS interface to link OpenGeoSys and MFront [3, 4].

2 Background

2.1 The theory of strength reduction

The term strength reduction implies that the classic strength parameters cohesion c, and friction coefficient $\tan\varphi$ of the slope soil are divided by a calculated reduction coefficient F_{trial}, producing a new set of c_{trial}, φ_{trial} values. It is then checked whether with these new values a static equilibrium can still be achieved. This process is repeated, i.e. F_{trial} is increased, until the slope soil becomes instable, i.e. deformations become large and no static equilibrium can be achieved. The corresponding limiting value of F_{trial} is the slope safety factor F_{s}. The strength reduction is described as the following equations:

$$c_{\mathrm{trial}} = \frac{c}{F_{\mathrm{trial}}} \tag{1}$$

$$\varphi_{\mathrm{trial}} = \arctan\left(\frac{\tan\varphi}{F_{\mathrm{trial}}}\right) \tag{2}$$

2.2 Criteria for judgment of slope stability

At present, there are several evaluation criteria for determining slope failure:

- The displacement characteristics of monitoring points are chosen as a criterion.
- Having a equivalent plastic area running continuously from the bottom to the top of slope is used as an indicator for slope failure.
- The global stiffness matrix approaches singularity.

3 Example

The example, taken from m a numerical study of PLAXIS2D [5], is used to verify the results obtained by using OpenGeoSys. The geometry of the model is presented in Fig. 1, which was built with GMSH software and includes 2484 linear triangular elements. The input parameters are taken from the research [5], which are listed in Table 1. The point **A** has been chosen as a monitoring point.

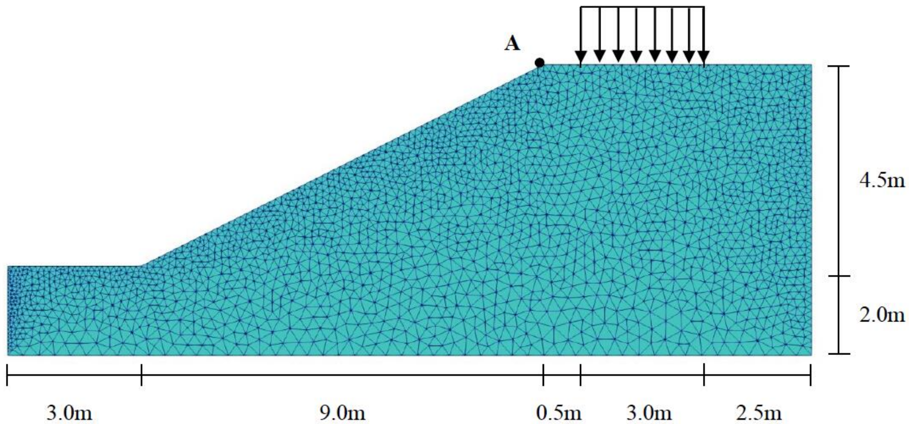

Figure 1: Model geometry and generated mesh.

The bottom boundary is fixed in all directions; the right and left boundaries are fixed in horizontal direction; the top load is applied along a length of $3\,\mathrm{m}$.

Table 1: The values of the material parameters

	Case 1	**Case 2**
Young's modulus (MPa)	2.6	2.6
Poisson's ratio	0.3	0.3
Density (kgm^{-3})	1600	1600
Cohesion (kPa)	5.0	5.0
Friction angle $(°)$	20	20
Dilatancy angle $(°)$	13	13
Tension-cuttoff value (kPa)	13.7	13.7
Top loading (kPa)	0	30

3.1 Numerical settings

The linear solver is used in this example is the BiCGSTAB solver from the Eigen library with an error tolerance of $1 \cdot 10^{-16}$ and a Diagonal preconditioner.

The non linear solver used is a Newton-Raphson scheme where the user specifies the maximum number of iterations (here 50) and a tolerance value for convergence control, here $1 \cdot 10^{-14}$ for the norm of the vector of increments of the unknowns.

The material model is integrated locally also with a Newton-Raphson scheme and a tolerance of $1 \cdot 10^{-14}$ for the residuals.

3.2 Time stepping

The time stepping is chosen as Table 2. The simulation is on the end when the slope is fairly close to the limit equilibrium state.

Table 2: Time stepping controlled by the number of non-linear iterations.

Time Start	0
Time End	6
Initial Δt	0.1
Minimum Δt	1×10^{-4}
Maximum Δt	0.5

3.3 Simulation procedure

In the Table 2, the simulation set-up is presented. In order to ensure the stability of the calculation, the gravity and the top loading are gradually increased to the maximum value. The phi-c reduction is from 3 s, as Eq. (1) and Eq. (2).

Table 3: Simulation set-up

	0 s	1s	2s	3 s	4 s	5 s	6 s	7 s
Density ($\mathrm{kgm^{-3}}$)	0	1600	1600	1600	1600	1600	1600	1600
Top loading (kPa)	0	0	30	30	30	30	30	30
Cohesion (kPa)	5	5	5	5	4.5	4	3.5	3
Friction angle (°)	20	20	20	20	18.12	16.24	15.26	12.32
Tension-cuttoff value (kPa)	13.7	13.7	13.7	13.7	13.7	13.7	13.7	13.7

4 Simulation results

4.1 Case 1 – Without top loading

Loss of convergence occurred once the reduction coefficient F_{trial} reached 1.534, so that $F_{\mathrm{s}} = 1.534$.

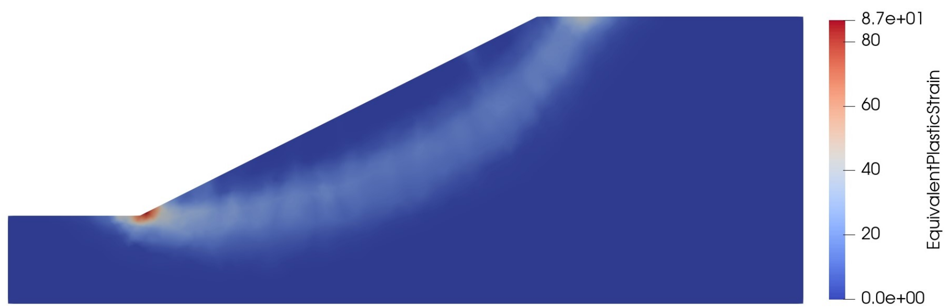

Figure 2: The equivalent plastic strain in Case 1

The distribution of the equivalent plastic strain is shown in Fig. 2, while the displacement magnitude and horizontal displacement component during the reduction step are displayed in Fig. 3 and Fig. 4, respectively. Fig. 2 clearly shows penetration of the slope by a plastic zone with the failure surface passing through the foot of the slope. At the same time, the displacement in the monitoring point Fig. 5 can be seen to increase drastically simultaneously with reaching the convergence limits because no static equilibrium can be found.

Thus we see that all of the criteria mentioned above are fulfilled simultaneously.

4.2 Case study 2 – With top loading

The final safety factor of $F_{\mathrm{s}} = 1.303$ was determined in OpenGeoSys.

The distribution of the equivalent plastic strain is shown in Fig. 6, while the displacement magnitude and horizontal displacement component during the reduction step are displayed in Fig. 7 and Fig. 8, respectively. Fig. 6 clearly shows

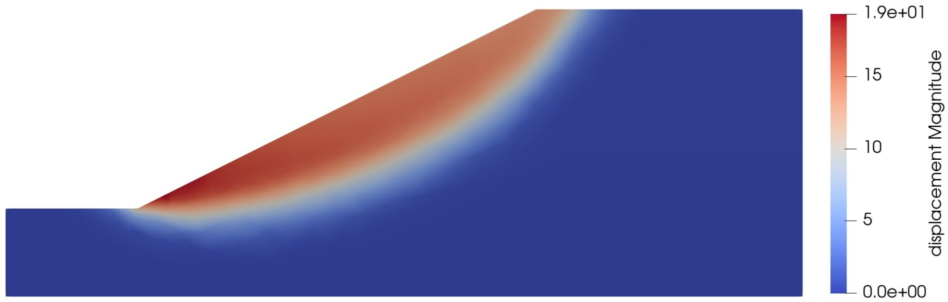

Figure 3: The displacement magnitude in Case 1 ($u_{\mathrm{m}} - u_{\mathrm{mg}}$). Here, u_{mg} is the displacement magnitude at the end of the gravity step.

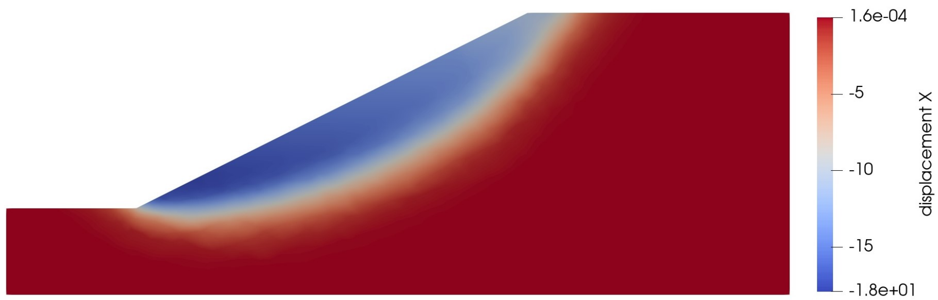

Figure 4: The horizontal displacement in Case 1 ($u_{\mathrm{x}} - u_{\mathrm{xg}}$). Here, u_{xg} is the horizontal displacement at the end of the gravity step.

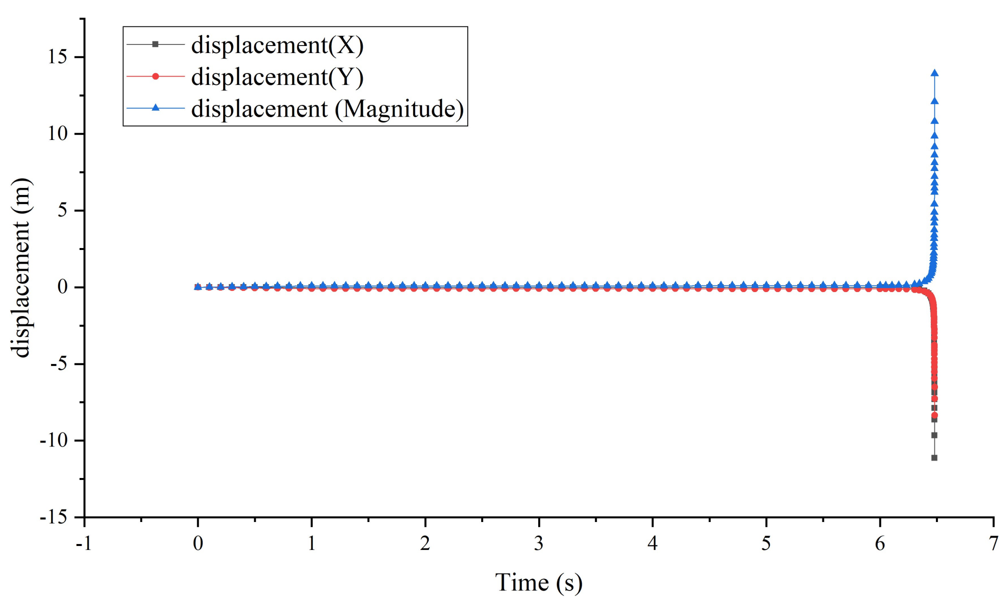

Figure 5: The displacement of the monitoring point A in Case 1

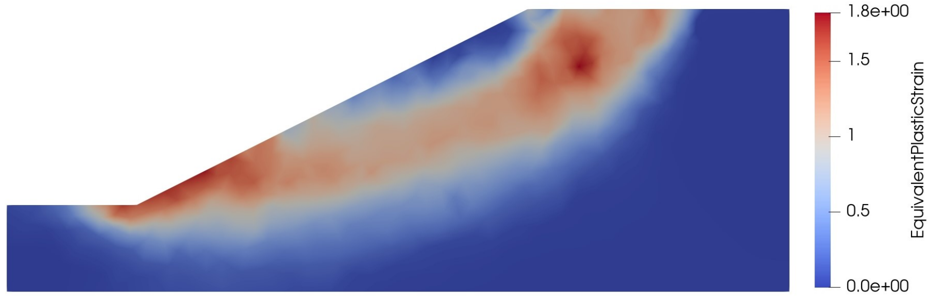

Figure 6: The equivalent plastic strain in Case 2

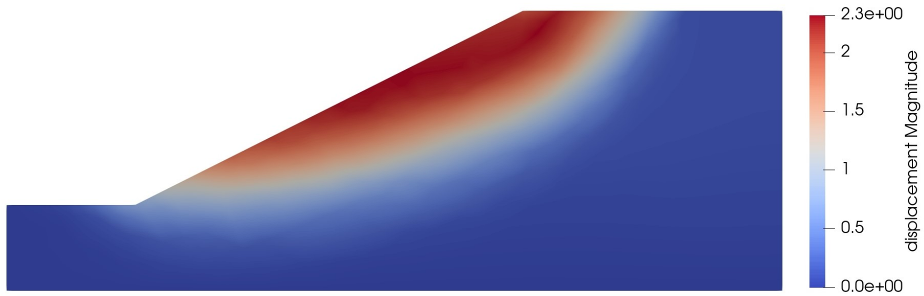

Figure 7: The displacement magnitude in Case 2 ($u_{\mathrm{m}} - u_{\mathrm{mg}}$). Here, u_{mg} is the displacement magnitude at the end of the gravity step.

penetration of the slope by a plastic zone with a slightly altered geometry of the failure surface compared to the previous case where only gravity was acting. At the same time, the displacement in the monitoring point Fig. 9 can be seen to increase drastically simultaneously with reaching the convergence limits because no static equilibrium can be found.

5 Verification

The safety factor calculated based on Bishop's limit equilibrium method is 1.534 for Case 1 [6], which is identical to the simulation results of OpenGeoSys. Plaxis2D yielded a safety factor of 1.540 in Case 1 [5] which is a difference of $0.4\,\%$ to the analytical and OGS result.

In Case 2, the Plaxis2D result was 1.261 [5] while OGS produced a value of 1.303, which is a difference of $3.4\,\%$.

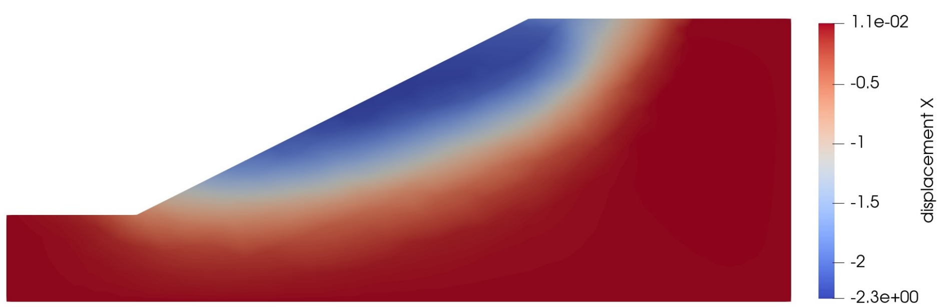

Figure 8: The horizontal displacement in Case 2 ($u_{\mathrm{x}} - u_{\mathrm{xg}}$). Here, u_{xg} is the horizontal displacement at the end of the gravity step.

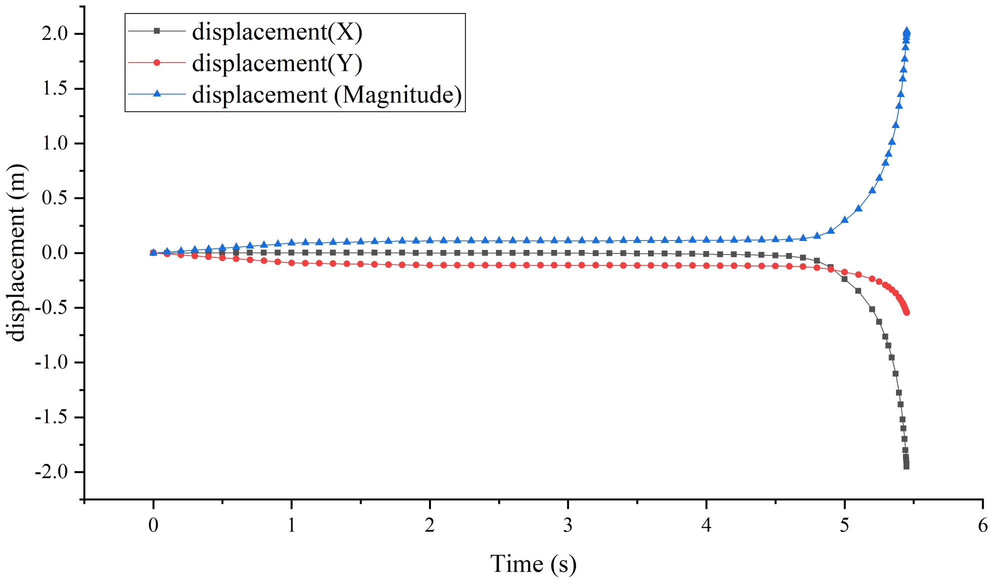

Figure 9: The displacement of the monitoring point A in Case 2

Looking at the result in Fig. 9, it seems that the slope hasen't reached as stringent a limit as seen in Fig. 5. Therefore, we perform the analyses shown in the next section to study the impact of numerical parameters.

6 Influence of numerical parameters

To study the impact of the discretization and the convergence criteria, the Case 2 analyses were repeated with slightly different settings:

- *Reference case:* $\|\Delta \mathbf{u}\| < 1 \cdot 10^{-14}\,\mathrm{m}$ $\Delta t_{\text{min}} = 1 \cdot 10^{-4}\,\mathrm{s}$, mesh from Fig. 1 with linear elements.
- *Refined mesh case:* $\|\Delta \mathbf{u}\| < 1 \cdot 10^{-14}\,\mathrm{m}$, $\Delta t_{\text{min}} = 1 \cdot 10^{-4}\,\mathrm{s}$, mesh with three times as many elements.
- *Higher-order mesh case:* $\|\Delta \mathbf{u}\| < 1 \cdot 10^{-14}\,\mathrm{m}$, $\Delta t_{\text{min}} = 1 \cdot 10^{-4}\,\mathrm{s}$, reference mesh with quadratic elements.
- *Nonlinear tolerance case:* $\|\Delta \mathbf{u}\| < 1 \cdot 10^{-10}\,\mathrm{m}$, $\Delta t_{\text{min}} = 1 \cdot 10^{-4}\,\mathrm{s}$, mesh from Fig. 1 with linear elements.
- *Minimal time step case:* $\|\Delta \mathbf{u}\| < 1 \cdot 10^{-14}\,\mathrm{m}$, $\Delta t_{\text{min}} = 1 \cdot 10^{-6}\,\mathrm{s}$, mesh from Fig. 1 with linear elements.

Table 4: The value of safety factor under different conditions. Plaxis 2D yielded a value of 1.261

Case	**Factor of safety**
Reference case	1.303
Refined mesh case	1.231
Higher-order mesh case	1.154
Nonlinear tolerance case	1.302
Minimal time step case	1.280

In Table 4 we summarize the results of the above case studies. The higher-order mesh case yielded a significantly lower F_{s} than the other cases, even lower than the reduction obtained by refining the mesh to three times as many elements. A higher F_{s} was obtained by increasing the non-linear tolerance. Furthermore, there is no significant difference between the reference case and the minimal time step case.

References

[1] A.J. Abbo and S.W. Sloan. A smooth hyperbolic approximation to the Mohr-Coulomb yield criterion. *Computers & Structures*, 54(3):427–441, feb 1995.

[2] Thomas Nagel, Wolfgang Minkley, Norbert Böttcher, Dmitri Naumov, Uwe-Jens Görke, and Olaf Kolditz. Implicit numerical integration and consistent linearization of inelastic constitutive models of rock salt. *Computers & Structures*, 182:87–103, apr 2017.

[3] Thomas Helfer, Bruno Michel, Jean-Michel Proix, Maxime Salvo, Jérôme Sercombe, and Michel Casella. Introducing the open-source mfront code generator: Application to mechanical behaviours and material knowledge management within the PLEIADES fuel element modelling platform. 70(5):994–1023.

[4] Thomas Helfer. A brief introduction to the MGIS c++ library for mechanical behaviours.

[5] Plaxis2D. Phi-C Reduction and Comparison With Bishop ' S Method Validation & Verification, 2012.

[6] Arnold Verruijt. *Soil Mechanics*. Delft University of Technology, 2006.